Thermal Studies of Synthetic NaX Zeolite and Its Zinc Exchanged Forms

[1]S. AKBAR* [2]T. H. SHAH, [3]R. SHAHNAZ, AND [4]G. SARWAR
[1]*Department of Chemistry, University of Balochistan, Quetta, Pakistan.*
[2]*Government Degree College, Pishin, Pakistan.*
[3]*Government Girls College, Quetta Cantt, Pakistan.*
[4]*Government Degree College, Sariab Road, Quetta, Pakistan.*

(Received 23rd April, 2006, revised 21st November, 2006)

Summary: NaX-Zeolite was converted to Zn forms by replacing sodium ions by zinc ions, amounting to a replacement from 16.60 % to 62.90 %. Chemical, TGA and DTA analysis of the zeolite samples was conducted and data on the composition of the unit cell (u.c.), zeolitic water and thermal stability of the lattices were obtained. The percentage of exchange of Zn^{2+} cations at 60 °C for a particular period decreased with increasing the concentration of Zn^{2+} cations in the exchange solution. The zeolitic water contents of NaX and ZnNaX zeolites were investigated by TGA up to 1000 °C. The TGA data indicated that all the samples of zeolites after dehydration underwent a small change in weight, occurring higher temperature due to dehydroxylation. The water content per u.c. was found to be larger in ZnNaX than in NaX. The TG curves of lumpy nature indicated the formation of a series of intermediate structures during dehydration. The minimum endothermic peak of dehydration shifted toward high temperature for ZnNaX zeolites suggested H_2O molecules to be more strongly bonded to Zn^{2+} cations than Na^+ cations. The slight shift of exothermic peaks of DTA towards high temperature indicated that ZnNaX zeolites are thermally more stable than NaX zeolite. The DTA curves indicated that dehydrated NaX retained its crystal stability from 370 to 580 °C and NaX and ZnNaX zeolites from 370-440 °C to 800 - 840 °C. NaX amorphized at ~ 960 °C and ZnNaX zeolites amorphized at 920-990 °C depending on the % of exchange of Na^+ ions. The results are discussed with respect to hydrated cations, possible sites they occupy in the zeolite framework, the effect of extra framework cations and Si / Al ratio on thermal stability.

Introduction

Zeolites have a very open framework with ultra fine pores of molecular dimensions in which extremely high surface areas are developed; sometimes 1000 $m^2 g^{-1}$ [1], being typically of the order of 300-700 $m^2 g^{-1}$ [2-3]. The zeolites finding the largest-scale application in catalysis belong to the family of faujasites including zeolite X and zeolite Y, having 0.74 nm apertures (12-ring) and a three dimensional phase structure. Their chief applications are in catalytic cracking of petroleum molecules, giving smaller, gasoline- range molecules [4]. The framework structure of zeolite X is formed by connecting each sodalite cage to four other sodalite cages; each connecting unit is made up of six bridging oxygen ions linking the hexagonal faces of sodalite units as shown else-where [5]. The bridging oxygens form what is called the hexagonal prism. There is a range of faujasite compositions, with typical units cell formula being [6]: $Na_j [(AlO_2)_j (Si O_2)_{192-j}]$. zH O, where j ranges from 96 to 74 for zeolite X and z drops respectively from about 270 to about 250 as Al decreases. The X-ray data determined the exact positions of cations present to balance the excess negative charge of the AlO_4 tetrahedra [7-9]. The exchangeable cations can be located at various sites [7].

The use of zeolites in the control of pollution, including effluents polluted with heavy metal ions [10-12], has recently increased [13-14]. Zeolites are appropriate materials for removing heavy cations from waste water because of their relatively low price coupled with the harmlessness of their exchangeable cations. Of the various zeolites available, synthetic X zeolites have an open, negatively charged framework [2]. The exchangeable cations located in super- and beta- cages, are easily accessible whereas, others, located in hexagonal prisms, have balancing cations, which are exchanged under extremely favorable conditions. The limiting dimensions of the apertures, which control access to these small cavities, are frequently given as a limiting factor of the ion exchange reaction. By applying suitable combinations of ion exchange, chemical

*To whom all correspondence should be addressed.

modifications and thermal activation procedures, zeolites have been tailored into suitable substrates for important industrial operations [2, 15-16].

The present work provides basic information on synthetic NaX and Zn types of X zeolites. It includes their chemical composition, the effect of various factors on % exchange, the zeolitic water and the thermal stability of the crystalline lattices. The zeolitic water was calculated by the % weight loss of the zeolite sample up to 1000 °C and the thermal stability was determined as a function of percentage exchange of Na^+ ions. We used the position of the exothermic peak in the DTA diagram to indicate lattice breakdown.

Results and Discussion

The five NaZnX zeolite samples having exchange levels of 16.60 %, 34.16 %, 37.27 %, 54.88 % and 62.90 % Na^+ replaced by Zn^{2+} ions were prepared by ion exchange technique given in Table-1 and were designated X/Zn (x) where x is the percentage of Na^+ exchanged by Zn^{2+}. The Table shows that in general, the percentage of exchange decreases as the concentration of $ZnCl_2$ solution increases. The factors responsible for this decrease are 'volume effect' [17], 'salt imbibent' [18-19] and 'concentration valency effect' [20]. These factors have been discussed in detail elsewhere [21].

Table-1:Preparation and analysis of Zn^{2+} exchanged X-zeolites

Zeolites	$ZnCl_2$ Mol dm^{-3}	Exchanged Zn^{2+} Cations %	No.of Na^+ cations released p.u.c+	Formulae p.u.c of anhydrous ZnNa X-Zeolites*
X/Zn (16.60)	0.0105	100	15.28	$Zn_{7.64}Na_{30.72}X$
X/Zn (34.16)	0.0204	99.02	29.40	$Zn_{14.70}Na_{56.60}X$
X/Zn (37.27)	0.0309	71.23	32.06	$Zn_{16.03}Na_{53.94}X$
X/Zn (62.90)	0.0396	93.94	54.10	$Zn_{27.05}Na_{31.90}X$
X/Zn (54.88)	0.0500	64.90	47.20	$Zn_{23.60}Na_{38.80}X$

+ p.u.c. (per unit cell) is used for convenience
* $X = [(AlO_2)_{86}(SiO_2)_{106}]^{86-}$

It is generally assumed that type X zeolite with the high charge density of its framework [Si/Al= 1.2] has a higher affinity for cations of higher charge. However, small divalent cations are highly hydrated to displace the Na^+ ion in the small sodalite cages, they must diffuse through a ring of six tetrahedra (6-ring), the diameter of which is 0.25 nm, which connect the sodalite cages and the super-cages. This requires partial dehydration of the ion's hydration shell. Consequently, a strong influence of the ionic radii on the exchange process is expected.

The typical thermograms of NaX and X/Zn (37.27) and DTA profiles are included for comparison purposes in Figs. 1 and 2, respectively. The thermograms of all zeolite samples studied were continuous and smooth and showed that dehydration started between 40 °C and 50 °C and the maximum percentage weight loss (23.78 to 29.29) occurred at about 370 – 440 °C and the dehydration completed at about 842 to 950 °C, depending on the number of Na^+ and Zn^{2+} ions p.u.c. of the zeolite sample. The relative data of thermal analyses are summarized in Table-2. The lumpy nature of TG curves probably results from the formation of a series of intermediate structures. The thermograms showed continuous loss of water with increasing temperature. This type of isobar is typical of a stable zeolite structure [6]. In zeolites that undergo dehydration reversibly and

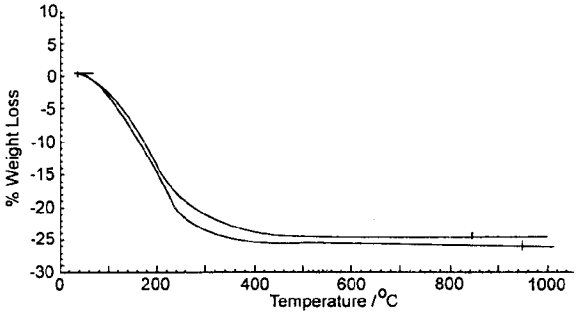

Fig. 1: Thermogra, of (a) NaX. and (b) X/Zn (37.27) zeolites.

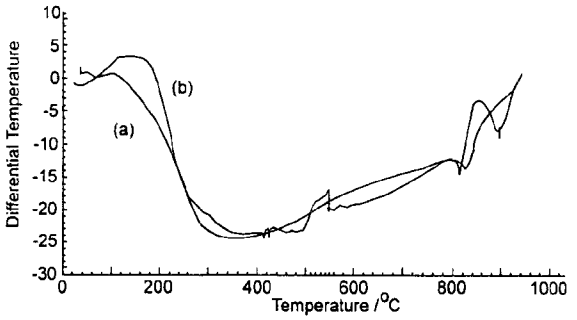

Fig. 2: DTA Profiles for (a) NaX and (b) X/Zn (37.27) Zeolites.

continuously, there is no substantial change in the topology of the framework structure. Exchangeable cations, located in the channels coordinated with water molecules may migrate to different sites, located on the channel walls or other positions of coordination. As zeolite X has several cation sites the effect of dehydration may be pronounced. The water molecules are present in clusters which seem to be

Table-2:Summary of thermal analyses data of NaX and ZnNaX zeolites

Zeolites	Loss in wt.%	Temperature °C of				Zeolitic water molecules p.u.c.
		Mini. of Endothermic peak of dehydration	Mini. of endothermic peaks of recrystallization	Completion of dehydration	Maxi. of exothermic peaks of crystal collapse	
NaX	23.78	370	585,880	842	580,850	232
X/Zn (16.60)	24.66	370	850	875	825	253.42
X/Zn (34.16)	25.47	380	825,860	900	800,840	257.45
X/Zn (37.27)	26.20	380	860,950	900	840,900	270.14
X/Zn (54.88)	26.38	440	845,940	900	820,890	273.18
X/Zn (62.90)	29.29	440	845,940	950	830,890	319.17

joined into a continuous intracrystalline phase. The zeolite is referred to as a nonstoichiometric hydrate because the water is present as a guest molecule in the host structure [6]. The TGA (Fig. 1) of NaX and Zn^{2+} substituted forms gave curves of similar shape and water loss occurred in stages in a wide temperature range (Table-2). Increasing substitution of Na^+ by Zn^{2+} in X zeolite causes the DTA curves to smooth out because of energy homogenization of adsorption centers.

The thermogravimetric curves in Fig. 1 correlate well with the DTA profiles in Fig. 2 and show that there are at least two types of water, mobile and immobile ones, in the narrow phase zeolites, while there is only mobile water in the wide pore zeolite [22]. The TGA curves showed that the maximum weight losses occurred at 280 °C for NaX and for ZnNaX zeolites at 280-340 °C, depending on the % of exchange of Na^+ ions by Zn^{2+} ions. This water is assumed to be sorbed and free mobile water inside the supercages and the water lost at above 280 °C was that forming hydration complexes with the cations and near the periphery of supercage tightly bonded to framework oxygens and in the small cages and pores of the zeolite samples. A slight weight loss in NaX at 842 °C and in ZnNaX zeolites at 875 to 950 °C may be due to dehydroxylation [15, 23]. For strongly polarizing cations, a water molecule yields a hydroxyl bonded to the cation plus a proton, which attaches itself to the framework oxygen (Ox^-). Ultimately as the temperature rises, the hydroxyls are destroyed with the expulsion of water

$$Zn(H_2O) + Ox^- \longrightarrow Zn(OH)^+ + OxH \quad (1)$$

$$2Zn(OH)^+ \longrightarrow Zn^+ - O - Zn^+ + H_2O \quad (2)$$

The reaction (1) does not occur until the $Zn^{2+}(H_2O)_n$ ions are dehydrated to the extent n=1, when the polarizing field of the partially unscreened Zn^{2+} is sufficient to dissociate the remaining water molecules. In general, the dehydroxylation of zeolites is slow and occurs in the temperature range of 500 – 800 °C [24]. It may not be accompanied by a distinct weight loss step in the TGA curve but it shows a slow and continuous weight loss up to 1 – 1.5 % in this range.

Table 2 indicates that NaX zeolite contains 232 water molecules p.u.c. whereas the literature reports it to be 243.6 [15] by weight loss at 800 °C and 257 [25] by weight loss at 600 °C and 264 H_2O p.u.c. [26]. The water content of NaX depends on the number of aluminum ions in the zeolitic framework [6]. The number of Al p.u.c. in NaX varies from 77 to 96. As the ratio Si/ Al decreases, the lattice constant of the zeolite increases slightly in accordance with the variation in Al - O (0.1728 nm) and Si - O [0. 1608 nm] distance and an increase in hydrophilicity. Water molecules interact with extra framework cations present in the zeolite and form hydrogen bonds with negatively charged oxygen ions associated with the zeolite lattice.

Table 2 indicates that the zeolitic water increases with the increasing degree of exchange. These results agree with those reported in the literature [25, 27]. Coughlan and Carrol reported 259.2 H_2O for NaX and 286 H_2O for X/Zn (80.8), Gal and Radovanov reported 257 H_2O for Na X and 273 H_2O p.u.c. for X/Zn (77.77) Zeolite. The zeolitic water increases with decrease in the cationic radius and increase in the valency of the cation [25, 27]. The size and number of cations in u.c. of a zeolite obviously affect the number of water molecules, which can be accommodated to p.u.c. of the zeolite. The Pauling's ionic radius of Na^+ is 0.069 nm and that of Zn^{2+} is 0.074 nm [25, 28]. As $2Na^+$ ions are replaced by one Zn^{2+} ion, therefore the space left vacant in the cavities is filled by water molecules,

which cause increase in zeolitic water. Thus, the amount of water adsorbed increases with the electric field of the cation i.e. inversely with the ionic radius [27, 29]. In a structure as rigid as X zeolite, the increase of water content also occurs by a closer packing of water molecules around the cations and that is exactly what the change of water concentration shows. Further, there is greater ordering of water molecules around the Zn^{2+} ions due to tetrahedrally coordinated Zn^{2+} i.e. the formation of Zn^{2+} $(H_2O)_4$ complexes in fully hydrated ZnNaX zeolite [25, 28, 30]. Table 2 shows that the number of H_2O molecules p.u.c. increases in the order X/ Zn (16.60) < X/ Zn (34.16) < X/ Zn (37.27) < X/ Zn (45.8) < X/ Zn (62.90).

In a hydrated zeolite, a small fraction of divalent cation can be expected to be located in site-I. In the case of complete exchange, the divalent ions predominantly occupy positions in the large cages in the initial phases of the exchange reaction, the sites in the small cages being taken in the very last stages of the exchange [31]. The temperature induced irreversibility, as observed by Maes and Cremer has been explained as a consequence of the difficulty for diva-lent ions to shed their water of hydration to enter (or leave) the small cages, being in accord with the views of Barrer [32] and Sherry [33]. In the samples of ZnNaX zeolite, the Zn^{2+} cations are contained in the supercages only [31]. The volume of the cations are important in determining the zeolitic water, since the u.c. volume of zeolite X, as determined by X-ray crystallography is 7.6 nm^3 p.u.c. for the supercage and sodalite cavities [29]. The higher negative charge density of the zeolite must produce a stronger interaction with the dipoles of water molecules. Lai and Rees [29] calculated the density of water of zeolite X to be 1.08 X 10^3 kg m^{-3} as compared to the normal density of water i.e. 10^3 kg m^{-3}. Zn^{2+} cations must interact strongly with the zeolitic water molecules to account for the quite dense packing of the water molecules. It was deduced [29] that 16 Na^+ ions in X zeolite were all present in site I. The sodalite cages in these zeolite samples must be free of cations and capable of accommodating the maximum possible number of water molecules.

The DTA curves (Fig. 2) provided data to the thermal stability of the zeolitic framework of the zeolite samples investigated. Usachev *et al.*, [34] studied (by TGA and DTA) the thermal transformation of zeolite X containing zinc nitrates and Yuan *et al.*, [35] characterized the materials by thermal analysis. The low temperature endotherm represented the loss of water, while the higher temperature exotherm represented the conversion of the zeolite to another amorphous or crystalline phase [36]. The endothermic curves of DTA pattern indicated a continuous loss of water over a broad range commencing from 40 to about 370 °C for Na X and 40 – 50 to 370 – 440 °C (Table-2) for ZnNaX zeolites. The increase in the minimum peak temperature of the DTA endotherm of dehydration of ZnNaX zeolites indicated that Zn^{2+} ions bind intra-zeolitic water more strongly than Na^+ ions. Activation energies of the dehydration process were calculated by Piloyan [37] and the results showed that the smaller the cation radius is (i.e. the stronger its field), the higher the activation energy. Thus, the data in Table 2 confirm that water is adsorbed more strongly on ZnNaX zeolites than NaX zeolite because the main endothermic effect is shifted toward higher temperatures for Zn^{2+} containing X zeolites.

Table 2 indicates the maxima of exothermic peaks temperatures, which correspond to the collapse of the crystalline zeolitic framework. The exothermic nature of the crystal collapse is attributed to the large amount of surface energy associated with the zeolite. As mentioned earlier in the introduction that zeolites have very high surface areas sometimes up to 1000 $m^2 g^{-1}$, so as the temperature of framework collapse, the surface area decreases and the energy associated with the host surface appears in the form of liberated heat [6]. The two exothermic peaks of NaX at 580 and 850 °C (Fig. 2) showed decomposition of the zeolitic lattice, followed by two maxima of endothermic peaks of recrystallization in a non-zeolitic form at 585 and 880 °C and at above 960 °C, the zeolite amorphized. Breck and Flanigen reported [38] that DTA exothermic peaks of NaX at 772 and 933 °C indicated the decomposition of the lattice, followed by the recrystallization to a new phase at 800 and 1000 °C. It has been reported [39] that most of the zeolitic water of NaX is lost by about 400 °C, but strong polarizations held the last water molecules tenaciously, keeping the thermal breakdown of NaX to be near 760 °C. Bravo *et al.*, reported on DTA curves that NaX amorphizes at 964 °C [ref. 15 P. 369]. Gal and Radovanov observed [25] a collapse of the zeolitic lattice by an exothermic peak for NaX at about 800 °C. The literature survey indicated that the different Si/ Al ratios of the zeolite were found to be responsible for the different thermal behavior [40].

The ultimate thermal stability of the zeolitic structure increased with increasing Si/ Al ratio for a given cation exchange form [41]. The stability of the crystal framework increases with increasing Si/Al ratios; decomposition temperatures of the different zeolites range from roughly 700 °C to 1300 °C [42]. Zeolites with high Si/ Al ratios are stable in the presence of concentrated acids, but those with low Si/ Al ratios are not; the trend is reversed for basic solutions. The temperature of structural decomposition of the zeolite and recrystallization decreases as the number of tetrahedral aluminum atoms in the framework increases, that is, as the Si/ Al ratio decreases. It has been observed that for Si/ Al ratio 2.4, the thermal stability was up to 810 °C and for Si/ Al ratio 6 up to 888 °C [41]. The breakage of Si–O (0.1608 nm) bond should require more activation energy than Al – O (0.1728 nm) bond. The cation density or the number of cations in the u.c. depends on the number of Al tetrahedral atoms in the framework and the stability appears to be related to the cation density and the framework charge [39].

The DTA data in Table 3 show that in general, the maxima of exothermic peaks of ZnNaX zeolites at 800– 840 °C and 825 – 900 °C indicate decomposition of the zeolite lattice, followed by maxima of endothermic peaks of recrystallization in another form at 825 – 860 and 850 – 950 °C and collapse to an amorphous residue at 920 – 990 °C, depending on the degree of exchange. The DTA data indicate that the maxima of exothermic peaks and temperature of complete amorphization of ZnNaX zeolites are higher than NaX zeolite, confirming the increased thermal stability of Zn^{2+} containing zeolites. The DTA curves indicate that the anhydrous phases of ZnNaX zeolites are stable up to 800 – 840 °C.

It has been reported [43-44] that thermal stability of zeolitic framework depends considerably on the types of cations, their distribution among the non framework sites and the degree of cation exchange. It has been attributed to the relation to the relative stability of the various cations to fill the voids within the crystal in the dehydrated zeolite [15, 39]. In general, cation exchange with multivalent cation and / or hydrogen enhances the thermal stability [45]. Some of the factors which influence the nature of the DTA curves include sample size of the specimen, heating rate and the atmosphere surrounding the specimen. The above results showed that chemical modification by ion exchange of X zeolite affects their physicochemical properties considerably. It has been confirmed that in the case of dehydrated ZnNaX zeolites, the Zn^{2+} ions are distributed preferentially in the hexagonal prisms and sodalite cages, forming $Zn(Ox)_n$ complexes where Ox is the lattice oxygen atom. The unit cell formulae of NaX and ZnNaX zeolite samples obtained from the data of Tables 1-3.

Table-3:Compositions of NaX and ZnNaX zeolites

Zeolites Unit	Cell Formulae
NaX	$Na_{86}\cdot[(Al\,O_2)_{86}\,(Si\,O_2)_{106}]\cdot 232\,H_2O$
X/Zn (16.60)	$Zn_{7.64}\,Na_{70.72}\cdot[(Al\,O_2)_{86}\,(Si\,O_2)_{106}]\cdot 253.42\,H_2O$
X/Zn (34.16)	$Zn_{14.70}\,Na_{56.80}\cdot[(Al\,O_2)_{86}\,(Si\,O_2)_{106}]\cdot 257.45\,H_2O$
X/Zn (37.27)	$Zn_{16.03}\,Na_{53.94}\cdot[(Al\,O_2)_{86}\,(Si\,O_2)_{106}]\cdot 270.14\,H_2O$
X/Zn (54.88)	$Zn_{23.60}\,Na_{38.80}\cdot[(Al\,O_2)_{86}\,(Si\,O_2)_{106}]\cdot 273.18\,H_2O$
X/Zn (62.90)	$Zn_{27.05}\,Na_{31.90}\cdot[(Al\,O_2)_{86}\,(Si\,O_2)_{106}]\cdot 319.17\,H_2O$

Experimental

All five samples of ZnNaX zeolites were prepared by the ion exchange procedure from synthetic NaX zeolite (lot # 96F0251) in powder form, binderless, purchased from Sigma (U.S.A). The following procedure to prepare X/Zn (54.48) (54.48 is the percentage of Na^+ exchanged for Zn^{2+} cations) zeolite sample is typical of the exchange methods used. Before Zn^{2+} exchange, NaX zeolite was stored in a desiccator over saturated calcium nitrate solution for complete hydration at ambient temperature. Sodium X zeolite (5 g) was slurried in 75 cm^3 deionized water and the pH reduced to 7 by the dropwise addition of hydrochloric acid (0.1 mol dm^{-3}) with constant stirring. A solution of $ZnCl_2$ (200 cm^3 0.0309 mol dm^{-3}) a lot # 4112775 (E. Merck) was added slowly with stirring and the mixture was stirred for a particular period at 60 °C. The slurry was filtered and the exchanged sample was washed several times with hot, deionized water (pH = 7.0). The wet samples were dried overnight at 80 °C and then stored over saturated calcium nitrate solution in a sealed desiccator for complete hydration. The compositions of the Zn exchanged samples, were checked by chemical analysis. The zinc content of the solution was analyzed before and after exchange by titration against 0.01 mol dm^{-3} EDTA (BDH, analar) had a lot # 9744320F with Erichrome Black-T (E.Merck, lot # 6376852) as indicator. Stoichiometric exchange occurred in all cases, since the amount of Zn^{2+} cations removed from solution was equivalent to the amount of Na^+ released from the zeolite. The X-type zeolites containing Zn^{2+} cations exchanged to different percentages are listed in Table-1.

Thermal analyses were carried out using a simultaneous thermal analyzer STA- 40 NETZSCH (Germany) 10-15 mg of each sample as prepared was taken using high purity nitrogen gas, a flow rate of 200 cm^3/ min was maintained over the sample, heating rate of 10 °C / min was employed and the chart speed was 2.5 mm/min. The zeolitic water was found by the % weight loss up to maximum temperature of 1000 °C and the thermal stability of the crystalline aluminosilicate framework was investigated by observing crystallinity changes at zeolite samples heated in the temperature range from room temperature up to 1000 °C.

Acknowledgements

The authors (G. S., T. H. S, and R. S) are indebted to the Education Department, Provincial Government of Balochistan, for grant of study leave and scholarship for doing M. Phil. T. H. S. and R. S. are thankful to Prof. Dr. M. Afzal the Ex-Dean of Natural Sciences, Quaid-i-Azam University, Islamabad and M. Arif of NMD, PINSTECH Nilore (Islamabad) for providing some research facilities.

References

1. J. B. Uytherhoeven, *Progr. Colloid and Polymer Sci.*, **65**, 233 [1978].
2. S. M. Auerbach, K. A. Carrado and P.K. Dutta, eds. Handbook of Zeolite Science and Technology, New York: Mercel Dekker, Inc. New York (2003).
3. S. Akbar and R.W. Joyner, *Jour. Chem. Soc; Faraday Trans. I*, 77, 803 (1981).
4. S. Akbar and S. Khatoon, *Sci. Tech. and Devel.*, **18**(4), 1 (1999).
5. S. Akbar, K. Dad, T. H. Shah and R. Shahnaz, *Jour. Chem. Soc. Pak.*, **28**(4), 317 (2006)
6. J. A. Rabo, ed., Zeolite Chemistry and Catalysis, *A. C. S. Monograph*, **171**, 3 (1976).
7. J. V. Smith, In: E. M. Flanigen, L. B. Sand, eds. Molecular Sieve Zeolites-I, A. C. S. Symposium Series, **101**, 173 (1971).
8. D. H. Olson, *J. Phys. Chem.*, **74**, 2758 (1970).
9. W. H. Bauer, *Am. Mineral.*, **49**, 697 (1964).
10. S. Akbar, *Sci. Tech. and Devel.*, **10**(3), 34 (1991).
11. B. Biskup and B. Subotic, *Sept. Sci. Technol.*, **39**, (4), 925 (2004).
12. D. Kallo, *Applications*, **45**, 519 (2001).
13. S. Chen; K. Chao and T. Lee, *Ind. Eng. Chem. Res.*, **29**, 2020 (1990).
14. B. Biskup and B. Subotic, *Sept. Sci. Technol.*, **35**(14), 2311 (2000).
15. D. W. Breck, In: R. P. Townsend, ed; The Properties and Applications of Zeolites, Special Pub. No. 33, The chemical Society, Lodon, 391 (1980).
16. J. Izumi, *Chem. Eng. (Tokyo)*, **41**, 557 (1996).
17. R. W. Barrer, L.V.C Rees and J. Shamsuzzona, *J. Inorg. Nucl. Chem.*, **28**, 629 (1966).
18. F. Hellferich, Ion Exchange, New York; McGraw Hill, 134 (1962).
19. R. M. Barrer and A. J. Walker, *Trans. Faraday Soc.*, **69**, 191 (1964).
20. R. M. Barrer and J. Kliowski, *J. Chem. Soc. Faraday Trans. I*, **70**, 2080 (1974).
21. S. Akbar, K. Dad, T. H. Shah and K. Shahna, *Jour. Chem. Soc. Pak.*, **27**(5), 456 (2005).
22. F. Ucon, *Z. Naturfors Sect. A.J. Phys. Sci.*, **57**(5), 281 (2000).
23. T. I. Barry and L. A. Lary, *J. Chem.. Phys.*, **50**, 4603 (1969).
24. H. A. Banesi, *J. Catal.*, **8**, 368 (1967).
25. I. J. Gal and P. Randovanov, *J. Chem. Soc. Faraday Trans. I*, **71**, 1671 (1975).
26. J. B. Uytterhoeven, *Colloid and Polymer Science*, **65**, 233 (1978).
27. B. Coughlan and W.M. Carrol, *J. Chem. Soc; Faraday Trans. I*, **72**, 2016 (1976).
28. T. A. Egerton and F.S. Stone, *J. Chem. Soc; Faraday Trans. I*, **69**, 22 (1973).
29. P. P. Lai and L.V.C. Rees, *J. Chem. Soc. Faraday Trans. I*, **72**, 1840 (1976).
30. A. Cremer In: J. R. Katzer, ed. Molecular Series-II, A.C.S. Symposium Series 40, *Am. Chem, Soc.*, Washington, 179, [1977].
31. A. Maes and A. Cremers, *J. Chem. Soc. Faraday Tans-I*, **71**, 265 (1975).
32. R. M. Barrer, J. A. Davies and L. V. C. Rees, *J. Inorg. Nuclear Chem.*; **31**, 2599 (1969).
33. H. S. Sherry, *J. Phys. Chem.*, **72**, 4086 (1968).
34. N. Y. Usachev, E. P. Belanuva, L. M. Krukousley, S. A. Kanaev, O. K. A. Kazakov, *Russ. Chem. Bull.*, **52**, 1940 (2003).
35. X. D. Yuan, J. Shen, G. H. Li, J. L. Zhou, J. M. Kim, P. S. Eon, *Chem. J. Chinese, Univ-Chinese*, **23**, 2332 (2002).
36. S. Chandrasekhar and P. N. Pramada, *Cerm. Int.* **28**, 177 (2002).
37. G. O. Piloyan, Introduction to the Theory of Thermal Analysis, Nauka, Moscow, (1964).
38. D. W. Breck and E. M. Flanigen, Molecular Sieves, Society of Chemical Industry, London,

47 (1968).
39. D. W. Breck, Zeolite Molecular Sieves, Structure, Chemistry, and Uses, Wiley Inter-Science, New York, (1974).
40. J. G. Martinez, D. C. Amaros and A. Z. Solano, *Langmuir*, **18**, 9778 (2002).
41. H. Bremer, W. Marke, R. Shödel and F. Vogt, In: W.M. Meier and J.B. Uytterhueven eds. Molecular Sieves, *Ad. Chem. Ser.*, 121, *Am. Chem.. Soc.* Washington, D.C. 249 (1973).
42. E. M. Flanigen, In: F. R. Ribeiro, A. E. Rodrigues, L. D. Rollmann and C. Naccache, eds. Zeolites: Science and Technology, Martinus Nijhoff, The Hague, 3 (1984).
43. R. A. Schoonheydt, L. J. Vandamme, P. A. Jacobs and J. B. Uytherhoeven, *J. Catal;* **43**, 292 (1976).
44. V. P. Shirakar and S. B. Kulkarni, *J. Thermal Anal.*, **25**, 399 (1982).
45. A. Godelitsas, D. Charislos, A. Tsipis, C Tsipis, A. Filippidis, C. Triantafyllidis, G. Manos and D. Siapkas, *Chemistry-A, European Journal*, 7(17), 3705 (2001).